Title

Probiotic therapy modulates the brain-gut-liver microbiota axis in a mouse model of traumatic brain injury.

Journal

Biochimica et Biophysica Acta (BBA) - Molecular Basis of Disease, 1870(8)

Authors

Amaral, Wellington
Kokroko, Natalie
Treangen, Todd
et al.

Publication Date

2024-12-01

DOI

10.1016/j.bbadis.2024.167483

Peer reviewed

HHS Public Access

Author manuscript

Biochim Biophys Acta Mol Basis Dis. Author manuscript; available in PMC 2024 December 01.

Published in final edited form as:

Biochim Biophys Acta Mol Basis Dis. 2024 December ; 1870(8): 167483. doi:10.1016/j.bbadis.2024.167483.

Probiotic therapy modulates the brain-gut-liver microbiota axis in a mouse model of traumatic brain injury

Wellington Z. Amaral[a,1], **Natalie Kokroko**[b,1], **Todd J. Treangen**[b], **Sonia Villapol**[c], **Fernando Gomez-Pinilla**[a,*]

[a] Departments of Neurosurgery and Integrative Biology and Physiology, University of California, Los Angeles, CA, USA

[b] Department of Computer Science, Rice University, Houston, TX, USA

[c] Department of Neurosurgery and Center for Neuroregeneration, Houston Methodist Research Institute, Houston, TX, USA

Abstract

The interplay between gut microbiota and host health is crucial for maintaining the overall health of the body and brain, and it is even more crucial how changes in the bacterial profile can influence the aftermath of traumatic brain injury (TBI). We studied the effects of probiotic treatment after TBI to identify potential changes in hepatic lipid species relevant to brain function. Bioinformatic analysis of the gut microbiota indicated a significant increase in the Firmicutes/Bacteroidetes ratio in the probiotic-treated TBI group compared to sham and untreated TBI groups. Although strong correlations between gut bacteria and hepatic lipids were found in sham mice, TBI disrupted these links, and probiotic treatment did not fully restore them. Probiotic treatment influenced systemic glucose metabolism, suggesting altered metabolic regulation. Behavioral tests confirmed memory improvement in probiotic-treated TBI mice. While TBI reduced hippocampal mRNA expression of CaMKII and CREB, probiotics reversed these effects yet did not alter BDNF mRNA levels. Elevated pro-inflammatory markers TNF-α and IL1-β in TBI mice were not significantly affected by probiotic treatment, pointing to different mechanisms underlying the probiotic benefits. In summary, our study suggests that TBI induces dysbiosis, alters hepatic lipid profiles, and preemptive administration of *Lactobacillus helveticus* and *Bifidobacterium longum* probiotics can counter neuroplasticity deficits and memory impairment.

* Corresponding author. fgomezpi@ucla.edu (F. Gomez-Pinilla).

[1] These authors contributed equally to this work.

Declaration of competing interest

The authors declare that they have no known competing financial interests or personal relationships that could have appeared to influence the work reported in this paper.

CRediT authorship contribution statement

Wellington Z. Amaral: Writing – review & editing, Writing – original draft, Methodology, Formal analysis, Data curation, Conceptualization. **Natalie Kokroko:** Writing – review & editing, Writing – original draft, Methodology, Investigation, Formal analysis, Data curation. **Todd J. Treangen:** Writing – review & editing, Supervision, Methodology, Formal analysis, Data curation. **Sonia Villapol:** Writing – review & editing, Supervision, Methodology, Formal analysis, Conceptualization. **Fernando Gomez-Pinilla:** Writing – review & editing, Supervision, Project administration, Investigation, Funding acquisition, Formal analysis, Conceptualization.

Appendix A. Supplementary data

Supplementary data to this article can be found online at https://doi.org/10.1016/j.bbadis.2024.167483.

Altogether, these findings highlight the potential of probiotics for attenuating TBI's detrimental cognitive and metabolic effects through gut microbiome modulation and hepatic lipidomic alteration, laying the groundwork for probiotics as a potential TBI therapy.

Keywords

Microbiota; Brain injury; Gut; Probiotics; Lipidomics

1. Introduction

Traumatic Brain Injury (TBI) is a severe neurological condition that often leads to long-term impairments in cognitive and neurological function. With approximately 1.7 million cases reported annually in the U.S., TBI represents a significant medical and social issue [1]. While most research on TBI has focused on its neurological aspects, the interaction between central and systemic physiology is poorly understood. Recent evidence suggests that the CNS plays a significant role in regulating systemic metabolism by influencing peripheral organ systems such as the gut, liver, and adipose tissue [2]. Therefore, the gut-brain-liver axis has been implicated in the physiological processes that regulate behavior, peripheral metabolism, systemic inflammation, and the pathogenesis of various diseases.

Multiple studies have shown that the effects of TBI extend beyond the CNS limits and can negatively impact gut and liver function, potentially worsening the TBI pathology. Brain injury results in blood-brain barrier (BBB) leakage, mitochondrial dysfunction, oxidative stress, accumulation of toxic neuropeptides, and impaired toxin clearance secondary to hepatic and renal dysfunction [3]. The gut's bacterial composition regulates metabolism, immune homeostasis, and brain function, and dysbiosis in the gut has been linked to inflammatory and metabolic disorders [4]. TBI patients frequently experience chronic gut dysfunction, and the commensal microbiota is a potent mediator in the gut-brain axis [5]. Therefore, targeted interventions of the gut microbiome are a promising avenue for preventing and treating host disease. The gut-liver-brain axis plays a crucial role in maintaining overall health and responding to physiological insults, with probiotic manipulations potentially offering protection and restoration [6]. Recent studies have suggested that certain bacterial strains, such as *Lactobacillus* and *Bifidobacterium*, may be necessary to prevent or lessen some digestive, inflammatory, metabolic, and neurological disorders [7–9]. *Lactobacillus helveticus* and *Bifidobacterium longum* have improved deficits in hippocampal plasticity, mood, and cognitive behaviors after neurological and psychological insults [10–16].

The liver, brain, and gut work in close collaboration, and the liver is responsible for processing absorbed nutrients, producing and metabolizing lipids, proteins, and hormones, and regulating glucose metabolism [17–20]. Our previous research has shown that moderate TBI can cause alterations in the metabolism and homeostasis of lipids in the liver in rodents [21,22]. Conversely, liver dysfunction can also impact brain health and further complicate the TBI pathology. The gut microbiota also plays a significant role in hepatic function and lipid homeostasis [23], suggesting that changes in hepatic metabolism after

TBI may be related to gut microbiota alterations and that probiotics may help mitigate TBI-induced changes in liver lipids [24]. Emerging evidence suggests that the gut-liver-brain axis orchestrates the whole body's nervous, enteric, metabolic, and immune function during health and in response to physiological insults. Thus, probiotic manipulations may protect the gut microbiota from TBI-induced disruptions, promote health, and restore balance in various physiological systems by harnessing the gut-liver-brain axis.

Our study employed a moderate Fluid Percussion Injury (mFPI) model to induce concussive brain injury in mice, which consistently induces changes in synaptic plasticity, central metabolism, and behavior [2]. We investigated the effects of this injury on the brain and memory of mice. We examined whether these changes were linked to alterations in gut microbiota and hepatic lipid profiles. Furthermore, we evaluated whether administering an oral probiotic formulation consisting of *L. helveticus* and *B. longum* could harness the influence of the gut microbiota to protect against both central and peripheral effects of TBI.

2. Material and methods

2.1. Animals

Twenty six-month old male C57/BL6 mice (Jackson Laboratories) were housed in polyacrylic cages and maintained under standard housing conditions (room temperature 22–24 °C) with a 12 h light/dark cycle. Cages and bedding material were replaced once a week, and the bedding material was mixed among all cages every two days to minimize the mice's exposure to communal fecal bacteria, thereby preventing co-housing effects. Previous studies have shown that co-housing may converge in-group microbiota profiles while significantly differentiating across social groups. A standard rat chow diet and water were supplied as ad libitum. Mice were divided into three groups through random assignment: Sham + control treated group (Sham; $n = 6$), brain injured + control treated group (TBI + Vh; $n = 7$), and brain injured + probiotic treated (TBI + Probiotic; n = 7) (Fig. 1). All experiments were performed in accordance with the United States National Institutes of Health Guide for the Care and Use of Laboratory Animals. The University of California at Los Angeles Chancellor's Animal Research Committee (ARC) approved animal studies and experimental procedures.

2.2. Microbiota manipulations

As recent studies show that probiotic interventions may have different effects on individual animals due to pre-existing microbiomes [25], we pre-treated mice with a short course of antibiotics to weaken and standardize their gut microbiomes as a baseline for subsequent probiotic and control treatments. Mice were administered with a broad spectrum poorly absorbable antibiotic combination (2 g/L streptomycin, 2 g/L bacitracin, and 0.5 g/L neomycin) in drinking water for 3 days before probiotic and control treatment (Fig. 1). These antibiotics were selected because they are poorly or non-absorbed by the gut, minimizing direct effects on the host or impairing glucose absorption in the gut. We chose short-duration antibiotic pretreatment based on the evidence that gut bacteria quickly adapt to continuous antibiotic treatments, losing efficacy in a few days. Following the antibiotic pretreatment, mice were switched to regular drinking water and treated with probiotics or

control. The probiotic formulation was comprised of freeze-dried *Lactobacillus helveticus R0052* and *Bifidobacterium longum R0175* (Probio'Stick®; Lallemand Health Solutions Inc., Canada), dosed at 10^9 CFU/mL each, dissolved in water (0.5 g/mL) for 0.2 mL oral gavage delivery. The control formulation comprised maltodextrin, Mg stearate, and milk powder (also provided by Lallemand Health Solutions Inc., Canada). The equal weight of the control was likewise dissolved in water (0.5 g/mL) for 0.2 mL oral gavage delivery. The probiotic and control solutions were administered by oral gavage daily between 3 days pre-surgery and 4 days post-surgery, and every other day until the animals were sacrificed at 14 days post-surgery (Fig. 1).

2.3. Fluid percussion injury (FPI)

FPI was performed as previously described [2]. In brief, animals were maintained in a deep anesthetic state during surgery using a Laboratory Animal Anesthesia System (VetEquip Inc., CA, USA). A 3.0-mm-diameter craniotomy was made over the left parietal cortex, 3.0 mm posterior to bregma, and 6.0 mm lateral (left) to the midline with a high-speed drill (Dremel, WI, USA). One moderate fluid percussion pulse (between 1.3 and 1.5 atm) was administered to the epidural space at the first sign of hind-limb withdrawal to a paw pinch. Sham animals underwent an identical preparation except for the lesion. FPI averaged 1.37 (SD = 0.15) atm pressure on the mouse cortex. Linear regression analyses of all experimental groups confirmed that fluid percussion pressure did not differ between TBI (M = 1.33, SD = 0.09) and untreated TBI (M = 1.39, SD = 0.19) groups ($F(2, 17) = 0.788$, $p = 0.387$). Similarly, there were no differences in recovery righting times (in seconds) after FPI between untreated TBI (M = 211, SD = 164) and probiotic-treated TBI (M = 245, SD = 178) groups ($F(2,17) = 0.190$, $p = 0.669$). Visual inspection of harvested brains also showed no light bruising of the cortical surface after FPI or sham surgery.

2.4. Behavioral assessments

2.4.1. Spatial learning and memory—The Barnes maze test was manufactured from acrylic plastic to form a disk 1.5 cm thick and 115 cm in diameter, with 40 evenly spaced 5 cm holes at its edges. Four overhead lamps were used as an aversive stimulus. Animals were trained to locate a dark escape chamber hidden underneath a hole positioned around the perimeter of a disk. All trials were recorded simultaneously by a video camera installed directly overhead at the center of the maze. Animals were trained with two trials per day for five consecutive days before being subjected to the experimental manipulations. A trial was started by placing the animal at the center of the maze covered under a cylindrical start chamber; after a 10s delay, the start chamber was raised. A training session ended after the animal had entered the escape chamber or when a predetermined time (5 min) had elapsed, whichever came first. Memory retention was tested during Barnes maze trials one week after injury (ten days after the probiotic intervention started). All surfaces were routinely cleaned with 70 % ethanol before and after each trial to eliminate possible olfactory cues from preceding animals.

2.4.2. Open field test—The open field test (OFT) provided information of the mice's locomotor activity and anxiety-like behavior [26]. The open field arena was a square (50 cm × 50 cm) with walls 40 cm high. Each mouse was placed individually in the center of

an open-field plexiglass box (60 × 60 × 20 cm), and its behavior was recorded for 10 min. The total distance traveled, and the cumulative time the mouse spent at the center of the arena were measured to assess anxiety-like behavior. Additionally, the percentage of time spent at the center (inner 25 % of the arena) versus the periphery (outer 75 % of the arena) was calculated to evaluate anxiety-like behavior. The arena was cleaned with 70 % ethanol between trials to remove scent cues.

2.5. Specimen collection

An inter-peritoneal glucose tolerance test (IPGTT) was performed on the eighth day post-surgery. On post-TBI day 10, animals were euthanized by decapitation, blood samples were obtained by cardiac venipuncture for plasma separation, and livers were dissected. Specimens were frozen in dry ice and stored at −80° until thawed for assays. Cecal microbial samples were also collected for microbiota analyses during the dissection, flash-frozen in liquid nitrogen, and stored at −80° until thawed for sequencing.

2.6. Glucose tolerance test

We performed the intraperitoneal glucose tolerance test (IPGTT) by the end stage (day 11 post-TBI) to study the effects of TBI and probiotic treatments on glucose metabolism. Mice were fasted for 16 h before a glucose tolerance test was performed. They were weighed, and basal blood samples were taken from the tail tip. Mice were injected intraperitoneally with glucose (dextrose at 2 g/kg), and further blood samples were taken at 15-, 30-, 60- and 120-min using glucometer (Bayer's Contour, NJ, USA) and glucose levels were measured.

2.7. Quantitative real-time PCR (qPCR)

The injury side of the hippocampus was rapidly dissected and immediately frozen in dry ice before being stored at −80 °C. Total RNA was isolated using the Direct-zol RNA MiniPrep kit (Zymo Research) per the manufacturer's protocol. The total RNA was converted to cDNA using PoweUp SYBR Green Master Mix kit (Applied Biosystems), and the mRNA was measured using High-Capacity cDNA Reverse Transcription Kit (Applied Biosystems) by the CFX96 Real-Time PCR Detection System (Bio-Rad). The GAPDH gene was used to standardize sample loading volumes as an endogenous control. The genes of interests were amplified by the following primer pairs: GAPDH (5′-CATGGCCTTCCGTGTTCCTA-3′, 5′-GCCTGCTTCACCACCTTCTT-3′), BDNF (5′-TGGCCCTGCGGAGGCTAAGT-3′, 5′-AGGGTGCTTCCGAGCCTTCCT-3′), CREB (5′-TGGAAGAACTGCACACGACA-3′, 5′-TCCCAGGATGGTTTGTTGGT-3′), CamKII (5′-TGGGTTTGGCTCTTGTATGGA-3′, 5′-AAGAAAACAGTGCAGACAGG AGATC-3′), TNF-alpha (5′-GCACAGAAAGCATGATCCGC-3′, 5′-CCCCAT CTTTTGGGGGAGTG-3′), IL1-beta (5′-ACTCCTTAGTCCTCGGCCA-3′, 5′-TGGTTTCTTGTGACCCTGAGC-3′), PPAR-gamma (5′-ATCTTAACTGC CGGATCCAC-3′, 5′-AGGCACTTCTGAAACCGACA-3′).

2.8. DNA extraction and long read 16S rRNA gene sequencing

DNA extraction and sequencing of the 16S ribosomal RNA gene were performed for mouse fecal samples as previously described by [27]. In brief, bacterial DNA was extracted

using the ZymoBIOMICS DNA kit (cat#D4300) with bead beating. The V4 region of the 16S gene was amplified and barcoded using 515f/806r primers, and then 250 × 2 bp sequencing was performed on an Illumina Miseq system. Raw sequence data were demultiplexed, then quality filtered and denoised with DADA2 [27] by trimming forward and reverse sequences off at 13 bases and truncating forward sequences at 249 bases and reverse sequences at 156 bases. All amplicon sequence variants (ASVs) were aligned with mafft [28] and used to construct a phylogeny using Fasttree [29]. Taxonomy was assigned to ASVs using the naïve Bayesian taxonomy classifier described in [30] against the Silva_nr_v132_train_set reference sequences from the Silva database. [2]. An average of 101966 (SD = 33325) sequences per sample were detected in the 16S sequencing data. After quality filtering, denoising, and merging, we obtained an average of 87824 (SD = 23899) non-chimeric sequences per sample, which were used for all microbiota analyses. There were no differences in sequencing depth across experimental conditions ($F(2,17) = 0.087$, $p = 0.917$).

2.9. Microbiota diversity indices generation

With the Amplicon Sequence Variant (ASV) generated from DADA2, Weighted UniFrac [31] and unweighted UniFrac [32] measures of beta diversity were generated in R using the phyloseq package. Principle Coordinate Analysis (PCoA) was done for both the weighted and unweighted Unifrac using the phyloseq object, which comprises the phylogenetic tree, the ASV tables from DADA2, and the metadata containing sample information. The statistical differences between the groups were analyzed using p values simulated by 999 permutations in ANOSIM. Also, Alpha diversity analyses were performed with Python v3.10.12 using the sci-kit biodiversity package v0.5.9. Three indices of alpha diversity were used to assess for sample richness and evenness: Simpson index (the species' relative abundance), Shannon index (richness and evenness), and Chao1 index (richness). The p values of these diversity metrics were calculated using one-way ANOVA to find the statistical differences between the TBI + Probiotic, TBI + Vh, and Sham conditions. UniFrac beta diversity measures identify differences in bacterial community structure or profile dispersion and composition. Weighted UniFrac accounts for the abundance of bacteria, while unweighted UniFrac accounts for the presence or absence of bacteria. Within-group 3D weighted and unweighted UniFrac PCoA plots were generated in R and used to identify group outliers beyond the boundaries of the group's 90 % ellipse error threshold.

2.10. Lipidomics

50–100 mg of tissue were collected in a tube pre-loaded with 2.8 mm ceramic beads (Omni #19–628). Tissue was homogenized with PBS in the Omni Bead Ruptor Elite (3 cycles of 10 s at 5 m/s with a 10-s dwell time), and 3–6 mg of homogenate was used for extraction [33]. Before biphasic extraction, a 13-lipid Lipidyzer Internal Standard Mix was added to each sample (AB Sciex, 5040156). Following two successive extractions, pooled organic layers were dried in a Genevac EZ-2 Elite. Lipid samples were resuspended in 1:1 methanol/dichloromethane with 10 mM Ammonium Acetate and transferred to robovials (Thermo 10800107) for analysis. Samples were analyzed on the Sciex Lipidyzer Platform for targeted quantitative measurement of 1100 lipid species across 13 classes. The differential Mobility Device on Lipidyzer was tuned with a SelexION tuning kit (Sciex 5040141). Data analysis

was performed on Lipidyzer software, and quantitative values were normalized to mg amounts used.

2.11. Comparison analyses

Group comparison analyses of behavioral and physiological measures and other specific variable analyses were carried out with the support package in R by linear regression modeling of ANOVA and multiple regression analysis for specific effect size estimates and, when appropriate, to adjust for multiple or covariate effects. Categorical variables were dummy-coded, where the TBI condition was coded (zero) as the reference group unless otherwise specified. This allows the specific assessment of whether differences can be detected between sham and untreated TBI mice and between untreated and treated TBI mice. The signs of regression coefficients were adjusted to reflect the directionality of effects. When necessary, natural logarithm transformation was applied to approach model assumptions of normality of the regression residuals. Fluid percussion pressure and mouse righting time after FPI were analyzed to mitigate confounding differences between TBI and TBI+ probiotic conditions. Locomotion was also tested to discriminate behavioral effects not due to differences in motor activity. Where appropriate, Benjamini-Hochberg's false discovery rate (FDR) correction was chosen to adjust for multiple testing effects in the omics experiments unless otherwise specified.

2.12. Differential abundance analyses of bacterial taxa

To analyze whether any of the conditions exhibited a significant difference in relative abundance, we carried out a multivariate association with linear models in MaAsLin2 (MaAsLin2, R package version 1.15.1) analysis [34] on the samples at the genus level. The taxonomic classification done by DADA2 was used as the input for the association studies. MaAsLin2 analysis aimed to uncover the microbial taxonomic differences associated with the three conditions (TBI + Probiotic, TBI + Vh, and the Sham). MaAsLin2 was run with its default parameters while having its fixed effects as the conditions of the samples. A 0.1 % and 1 % threshold were set for the minimum prevalence and minimum abundance, respectively. This filtering step was applied to focus the analysis on more abundant features. Boxplots were generated to visualize the relative abundance of the genus in each condition. To ascertain the statistical significance of these abundances and plots, raw *P* values, P-adjusted values (q value), and FDR (False Discovery Rates) were generated for each condition against the reference level specified, the Sham in Maaslin2. Finally, taxonomic abundance information was used to generate stacked bar plots at the phylum level to estimate the relative abundance among the three experimental conditions.

2.13. Assessing the impact of TBI on hepatic lipid profiles through multivariate analyses

Principal Component Analyses (PCA) analyses were performed in R to assess whether there were global differences in hepatic lipid profiles across the experimental conditions. We also used the principal component results to test whether the experimental conditions caused constrictions of global lipidomic profiles. Depending on whether each PCA component data was normally distributed and the degree of departure from normality, assessed by the Shapiro test and visually, we used Bartlett's test (parametric), Levene's test (parametric but less sensitive to departures from normality) or Fligner-Killen test (non-parametric) to

assess the homogeneity of variances. While PCA analyses maximize variance, Partial Least Square (PLS) is a preferred method of multivariate dimension reduction that maximizes the covariances within datasets. A PLS approach to Discriminatory Analyses (DA) allowed us to assess the discriminating features that differentiate the three experimental conditions based on specific subsets of lipids. Further, we used a spare PLS-DA, which imposes a penalization, removing uninformative variables and allowing for variable selection, thereby identifying potential physiological biomarkers. sPLS-DA implementation in the MixOmics R package was performed to identify differences in hepatic lipids by assessing the differential enrichment of lipids that characterize each experimental condition. Before sPLS-DA, the hepatic lipid data was preprocessed: lipids missing 10 % or more of data were removed; lipids missing at <10 % were imputed using nipals; and lipids exhibiting near-zero variances were removed. After preprocessing the data, PLS-DA models were generated, evaluated, and tuned with the Mfold validation method using 5-fold cross-validation repeated 100 times, and balanced and overall error rates were assessed using Mahalabonis distances. The DA components of the final optimized PLS-DA model were used for comparison and downstream analyses. Further, association analyses were carried out between hepatic lipids enriched in each condition and the microbiota taxa at the genus level.

3. Results

3.1. Probiotic treatment prevents memory deficits after brain injury

The total latency time (time to enter the escape box) in the Barnes Maze revealed differences in memory recall across conditions (ANOVA; $F(2,17) = 4.6447$, $p = 0.0246$). Specifically, untreated TBI mice exhibited greater latency times compared to sham mice ($\beta = 56.67$, $F(2,17) = 7.156$, $p = 0.016$), while probiotic-treated TBI mice exhibited lower latency compared to untreated TBI mice ($\beta = -52.79$, $F(2,17) = 7.098$, $p = 0.016$) (Fig. 2a). The OFT yielded no differences in spontaneous locomotor activity levels (total distance traveled) between groups (ANOVA; $F(2,17) = 1.491$, $p = 0.253$). These results suggest that cognitive performance measures were not confounded by possible effects of concussive injury on locomotor activity levels. In the OFT, we also analyzed the percentage of time spent by the mice in the center of the arena as a measure of anxiety-like behavior. There were no significant differences in the time spent in the center among the sham, untreated TBI, and probiotic-treated TBI groups (sham vs. untreated TBI, $\beta = -2.783$, $F = 0.080$, $p = 0.7809$; and untreated TBI vs. probiotic-treated TBI, $\beta = -6.104$, $F = 0.439$, $p = 0.5165$).

3.2. Effects of probiotic treatment on glucose metabolism

We determined whether probiotic administration would influence the action of TBI on systemic glucose metabolism. Mice subjected to TBI showed a trend to impaired glucose metabolism and slowly metabolized glucose compared to sham vehicle controls (Fig. 2b). The TBI-probiotic mice showed lower plasma glucose levels than the TBI-Vh group (Fig. 2b). There were no differences in body weight across the different groups and time points (data not shown). It is reasonable to assume that the observed changes in glucose metabolism are aggravated by TBI pathogenesis. One-way ANOVA with Tukey's multiple comparison test (*$p < 0.05$, **$p < 0.01$), $n = 6$–8/group.

3.3. Probiotic treatment counteracted the TBI-induced reduction in hippocampal mRNA levels of the plasticity markers CaMKII and CREB

We found group differences in BDNF mRNA (ANOVA; $F(2,17) = 4.126$, $p = 0.036$), CaMKII mRNA (ANOVA; $F(2,17) = 23.221$, $p < 0.001$), and CREB mRNA (ANOVA; $F(2,17) = 14.621$, $p < 0.001$) and across conditions (Fig. 3a–c). Specifically, TBI reduced levels of CamKII mRNA ($\beta = -4.419$, $F(2,17) = 46.383$, $p < 0.001$) and CREB mRNA ($\beta = -2.240$, $F(2,17) = 29.060$, $p < 0.001$) while probiotic treatment exerted reverse effect on both CaMKII mRNA ($\beta = 2.134$, $F(2,17) = 12.811$, $p = 0.003$), and CREB mRNA ($\beta = 1.266$, $F(2,17) = 10.010$, $p = 0.006$). TBI also decreased the mRNA levels of BDNF ($\beta = 0.42$, $F(2,17) = 0.153$, $p = 0.014$), however probiotic treatment did not affect BDNF mRNA levels ($F(2,17) = 0.147$, $p = 0.474$).

3.4. Probiotic treatment did not affect the TBI-related increases in hippocampal proinflammatory TNF-α and IL1-β and the metabolic-related PPAR-ɣ

We detected group differences in mRNA levels for TNF-α (ANOVA; $F(2,17) = 21.853$, $p < 0.001$) and IL1-β (ANOVA; $F(2,17) = 17.546$, $p < 0.001$), as well as for PPAR-ɣ (ANOVA; $F(2,17) = 4.711$, $p = 0.025$). There were greater hippocampal mRNA levels of TNF-α and IL1-β ($\beta = 2.32$, $F(2,17) = 22.047$, $p < 0.001$ and $\beta = 2.32$, $F(2,17) = 20.678$, $p < 0.001$, respectively) in untreated TBI mice, compared to sham controls (Fig. 3d–f). There also were greater PPAR-ɣ mRNA levels ($\beta = 1.66$, $F(2,17) = 7.339$, $p = 0.016$) in the hippocampus. However, the probiotic treatment did not prevent level changes in TNF-α and IL1-β mRNAs ($F(2,17) = 2.378$, $p = 0.143$ and $F(2,17) = 0.785$, $p = 0.389$, respectively), nor PPAR-ɣ mRNA ($F(2,17) = 0.030$, $p = 0.8655$).

3.5. Impact of probiotic treatment on gut microbiota diversity and composition in a mouse model of TBI

In the effects of probiotic treatment on gut microbiota diversity and composition in a mouse model of TBI, distinct microbial community dynamics were observed. Principal coordinates analysis (PCoA) based on Weighted UniFrac distances demonstrated clear segregation of microbiota communities among Sham, TBI-Vh, and TBI-Probiotic, as seen in the abundance of bacteria, weighted (Fig. 4a, $R = 0.3325$, $p = 0.001$) and in global bacterial profiles in terms of the presence or absence of specific bacteria, unweighted (Fig. 4b, $R = 0.3196$, $p = 0.001$) plots. POC analyses revealed that the probiotic treatment prevented the effect of brain injury on the number of observed OTUs: untreated TBI-Vh mice exhibited lower richness than sham control and TBI-Probiotic mice ($\beta = -22.94$, $F(2,17) = 4.986$, $p = 0.039$) with no difference between sham and TBI-Probiotic groups ($\beta = 0.88$, $F(2, 17) = 0.006$, $p = 0.939$) (Fig. 4c, $*p < 0.05$). Despite these differences in richness, the biodiversity indices, including the Simpson index (Fig. 4d, $p = 0.727$) and the Shannon index (Fig. 4e, $p = 0.303$), along with the Chao1 estimator (Fig. 4f, $p = 0.101$), indicated no significant variations in biodiversity across the groups. Moreover, the relative abundance profiles of major bacterial phyla (Fig. 4g) were dominated by *Firmicutes* and *Bacteroidetes* in all groups. However, the *Firmicutes/Bacteroidetes* ratio was significantly higher in the TBI-Probiotic group than in the TBI-Vh and Sham groups (Fig. 4h, $*p < 0.05$). This increase in the *Firmicutes/Bacteroidetes* ratio following probiotic treatment suggests a specific alteration in

gut microbiota composition, which could have implications for the gut-brain axis and the overall health of the TBI mice.

3.6. Changes in bacterial genera following probiotic treatment and traumatic brain injury

Following experimental TBI, we characterized the mouse gut microbiome using 16S rRNA full gene analysis of multiple stool samples. During our investigation into how the gut microbiome reacts to probiotic treatment (initiated three days before TBI and maintained for ten days after TBI), we discovered notable changes in the composition of bacterial genera. Fig. 5 displays the relative abundance of these bacteria across three different groups: Sham, TBI-Vh, and TBI-Probiotic mice. The abundance of *Turicibacter* was significantly elevated in the Sham group compared to the TBI-Vh and TBI-Probiotic groups (Fig. 5a, $*p < 0.05$, $**p < 0.01$). Similarly, *Acetatifactor* levels were higher in the TBI-Probiotic group compared to the Sham group (Fig. 5b, $*p < 0.05$). At the same time, *Marvinbryantia* and *Roseburia* showed no substantial variation across the groups (Fig. 5c and d). *Ruminiclostridium* was more abundant in the Sham group relative to the TBI-Vh and TBI-Probiotic groups (Fig. 5e, $*p < 0.05$, **p < 0.01), and *Lachnospiraceae* levels were notably increased in the TBI-Probiotic group (Fig. 5f, $****p < 0.0001$). *Ruminococcaceae* was more prevalent in the Sham group compared to the other two groups (Fig. 5g, *p < 0.05, **p < 0.01), while *Bifidobacterium* levels remained consistent across all groups (Fig. 5h). The abundance of *Lactobacillus* was higher in the TBI-Probiotic group than in TBI-Vh but did not differ significantly from the Sham group (Fig. 5i). *Butyricicoccus* increased in the TBI-Probiotic group compared to the TBI-Vh and Sham groups (Fig. 5j, *p < 0.05). *Akkermansia* was significantly reduced in the Sham and TBI-Probiotic groups compared to the TBI-Vh group (Fig. 5k, *p < 0.05). Lastly, the levels of Clostridium were dramatically decreased in the TBI-Probiotic group relative to both the Sham and TBI-Vh groups (Fig. 5l, ****p < 0.0001). These findings suggest that probiotic treatment can modulate the gut microbiome in the TBI condition, potentially influencing recovery and health outcomes.

3.7. TBI caused an alteration of overall lipidomic signatures

Fig. 6 underscores the effectiveness of Sparse Partial Least Squares Discriminatory Analysis (sPLS-DA) in detecting and visualizing variations in hepatic lipid profile resulting from TBI and probiotic pre-treatment. Each point on the plot corresponds to an individual sample's lipid profile, projected onto two principal components that elucidate 7 % and 9 % of the variance, respectively. The first component effectively discriminates between sham-operated (blue) and probiotic-treated (green) mice, whereas the second component distinctly separates the TBI vehicle-treated (red) mice. The clustering within the plot's ellipses, representing the 95 % confidence interval for each group, underscores the unique lipid signatures and the minimal overlap between them, showcasing the clear lipidomic divergence among the groups. The first component suggests that the probiotic intervention yields a lipidomic sub-profile distinct from the sham and TBI vehicle-treated conditions. The second component, accounting for a substantial portion of the variation, further delineates the effects of TBI and the probiotic treatment. Two principal components summarized the hepatic lipidomics data, PC1 and PC2, accounting for 46 % and 21 % of the variance, respectively (Supplemental Fig. 1). Fligner-Killeen or Levene's test for homogeneity of variances was used based on Shapiro's test for data normality. Based on the Fligner-Killeen test, there were no group

differences in the homogeneity of variances in the PC1 lipid subset ($\chi^2 = 0.647$, df = 2, $p = 0.724$; Shapiro's test, W = 0.743, $p < 0.001$). However, the analysis of PC2 by Levene's test revealed differences in the homogeneity of lipid profiles that are summarized by PC2 ($F(2,17) = 3.828$, $p = 0.042$; Shapiro's test, W = 0951, $p = 0.387$), indicating a constriction of lipid profiles in the TBI condition (red ellipse in Supplemental Fig. 1) relative to sham and probiotic treated groups.

3.8. TBI-induced shifts in specific hepatic lipid species, some of which were differentially altered by the probiotic treatment

sPLS-DA analysis revealed specific effects of TBI and probiotic treatment on lipid species in the liver. The optimized sPLS-DA model exhibited 2 components (sPLS-DA Components 1 and 2) used for downstream analyses. Table 1 presents the hepatic lipids that contribute significantly to each condition (magnitude of DA score ≥ 0.10). The sPLS-DA Component 1 identified 27 lipids (Supplemental Fig. 2). The experimental conditions constituted 82.6 % of the sPLS-DA Component 1 variance. They revealed the effects of TBI and probiotic treatments ($\beta = -2.68$, $F(2,17) = 13.933$, $p = 0.002$ and $\beta = -3.28$, $F(1,12) = 24.030$, $p < 0.001$, respectively), discriminating the lipids that characterized sham and probiotic treated animals. This analysis further revealed that the probiotic treatment did not return the lipid profile induced by TBI to the sham-like state but instead induced a lipid profile distinct from both sham and TBI groups (Fig. 4). The sPLS-DA Component 2 identified 102 lipids (Supplemental Fig. 3). The experimental conditions constituted 47.0 % of the variance in the sPLS-DA Component 2. Also, they revealed the effect of both TBI and probiotic treatment in opposite directions and similar magnitude ($\beta = -5.76$, $F(1,10) = 9.508$, $p = 0.007$ and $\beta = 6.4$, $F(1,12) = 13.275$, $p = 0.002$, respectively). This analysis discriminated the lipids that characterized the TBI condition and revealed a set of lipids that were affected by TBI and returned to a sham-like profile by the probiotic treatment.

4. Discussion

The action of gut microbiota in regulating host health and the progression of chronic disorders is becoming increasingly recognized. Gut microbiome-targeted interventions represent a promising venue to prevent and treat host disease. Results showed that TBI impacts gut microbiota diversity and composition, induced memory deficits, decreased neuroplasticity markers, and increased neuroinflammatory markers. Probiotic treatment with *Lactobacillus helveticus* and *Bifidobacterium longum* changed the gut microbiota composition in mice. The protective effects of the *Lactobacillus helveticus* and *Bifidobacterium longum* probiotic formulation on hippocampal plasticity, mood and cognitive behaviors have been examined in the context of other neurological and psychological challenges [35]. This formulation has also been shown to reduce neuroinflammatory status and hippocampal apoptosis [36] in various stressors. In addition, TBI promoted alterations in the profile of hepatic lipid species associated with specific gut bacteria species. Our data showed that the same probiotic treatment increased SCFA-producing bacteria in the gut, reshaped the lipid species profile, counteracted memory deficits in the Barnes maze, and disrupted molecular markers of learning/memory in the hippocampus.

Consistent with prior research [37,38], our results showed that the FPI model for concussive brain injury was efficient to induce memory deficits in mice and to decrease the expression of neuroplastic genes in the hippocampus [39]. In the current study, TBI reduced the expression of critical genes associated with hippocampal plasticity (BDNF, CREB, and CaMKII) and increased the expression of genes related to neuroinflammation (TNF-α and IL-1β) and metabolism (PPAR-γ). Elevated expression of PPAR-γ suggests a compensatory response to regulate cellular metabolism by decreasing triglycerides, increasing insulin sensitization, and counterbalancing the pro-inflammatory response [40]. Our results showed that the CREB/CaMKII signaling pathway was the most susceptible to the effects of the probiotics on memory performance. While the probiotic treatment did not elicit significant changes in TNF-α, IL-1β, or PPAR-γ levels, we cannot discard the possibility that neuroinflammatory events can influence neuroplastic processes [41].

It has been suggested that *Lactobacillus helveticus* and *Bifidobacterium longum* probiotic formulation can affect the brain and behavior through several mechanisms, including changes in glucose metabolism, one-carbon metabolism, and direct SCFA effects on cellular metabolic systems. Many studies suggest that SCFAs, especially butyrate, are significant mediators of the contribution of the gut microbiota to CNS health and behavior [42]. They may act through many pathways affecting cellular metabolism and eliciting major epigenetic reorganization.

Analyses of the gut microbiota beta diversity indicated significant differences in microbial profiles across sham, TBI-treated, and untreated animals, in which TBI predominantly affected the abundance of the existing bacteria. In addition, the probiotic treatment also generated an overall distinct microbiota profile, comprised of differences in both the abundance and presence of bacteria. Our findings align with current reports that the bacteria from probiotics do not necessarily colonize the intestine in a detectable manner [43]. Instead, probiotics can exert beneficial effects through transient interactions with the gut microbiota and the host's immune and metabolic systems. These effects were reflected in the total number of observed bacteria, a measure of specimen richness, which was reduced among the TBI mice and returned to normative levels by the probiotic treatment. Greater richness in the gut microbiota is generally accepted as beneficial, while a reduction, as seen in the untreated TBI condition, is often characteristic of abnormal or dysbiotic [44]. TBI reduced microbiota richness and the probiotic treatment restored the richness of the microbiota, albeit with different bacterial composition and abundance. In addition, these analyses indicate that TBI affected the abundance of the bacteria in the microbiota (weighted Unifrac) without eliminating or eliciting the formation of novel bacteria (unweighted Unifrac) relative to the sham animals. On the other hand, the probiotic treatment promoted changes in the abundance of existing bacteria and the presence and/or absence of other bacteria. Our study has several limitations: Firstly, the 16S gene analysis cannot offer strain-level information about the bacteria within the sample. Secondly, the complete 16S protocol employs primers that exhibit known biases [45]. Finally, there may be challenges in extrapolating the findings from the murine model to humans.

Administering these probiotics to animals in the TBI condition resulted in an increase of three distinct bacterial genera: *Acetatifactor*, *Lachnospiraceae,* and *Butyricicoccus,*

which are known SCFA producers in the *Clostridiales* order and appoints the direction to future studies in this model. *Lactobacillus helveticus* and *Bifidobacterium longum* themselves were not found among the gut bacteria promoted by the probiotic treatment, in agreement with reports that probiotics can promote a healthy microbiota without necessarily colonizing the gut microbiome [42]. Probiotics can exert beneficial effects through transient interactions with the gut microbiota and the host's immune and metabolic systems. For example, probiotics can modulate the existing gut microbiota by creating a more favorable environment for beneficial bacteria through competitive exclusion and production of antimicrobial substances [41]. These mechanisms, among others, have been posed to explain the observed benefits of probiotic strains despite the absence of detectable colonization. Our analysis revealed that *Roseburia,* though not statistically significant, and *Akkermansia* were the only two bacterial genera that showed differences between the sham and TBI groups, and their levels were normalized to sham levels upon probiotic treatment. *Akkermansia* is known to be involved in the generation of short-chain fatty acids (SCFAs), which play a crucial role in gut health and metabolic regulation [46]. The ability of *Akkermansia* to produce SCFAs suggests a potential mechanism through which probiotic treatment may exert its beneficial effects on gut and liver metabolism. This normalization of *Akkermansia* levels could contribute to the restoration of SCFA-mediated signaling pathways disrupted by TBI, thereby supporting the overall health of the host. It is also noteworthy that LefSE enrichment analysis indicated that most bacterial alterations occurred within the *Clostridiales* order (*Firmicutes* phylum), which is generally commensal in nature. However, this order was differentiated across experimental groups at the genus level.

TBI and probiotics affected lipid species with strong potential for cerebral function and plasticity [35]. These results point to a possible mechanism by which the probiotic-induced reshaping of the gut microbiota may have exerted protective effects on peripheral and central physiological systems, ultimately preventing the memory deficit provoked by TBI. The liver is an important source of lipids to be used throughout the body and brain. Lipids play crucial roles in energy metabolism, immune function, hormonal and cell signaling, acting across all organ systems, including the CNS [47]. Our results showed that TBI impacts the lipidomic profile of the liver and that the probiotic treatment protected the liver against several of these TBI-induced alterations (Fig. 6). Specific lipid profile analyses showed two subsets of hepatic lipids affected by TBI and the probiotic treatment. The first subset of hepatic lipids, comprised of 102 lipid species (sPLS-DA Component 2), showed an effect of TBI that was reversed by the probiotic treatment. The second subset of hepatic lipids comprised 27 species (sPLS-DA Component 1). Among the hepatic lipids that exhibited the most significant enrichment in the untreated TBI condition, we found cholesterol esters (CE), phosphatidylethanolamines (PE), phosphatidylcholines (PC), lysophosphatidylcholine (LPC) and triglycerides (see Table 1). Increases in these hepatic lipids are consistent with their roles in liver dysfunction, inflammation, and, most interestingly, brain degeneration, which can have enormous implications for controlling TBI pathogenesis. LPC is a significant component of oxidized low-density lipoprotein produced by the liver by hydrolysis of PC [48]. LPC may also act as a fatty acid carrier for other tissues, including the brain [49]. LPC pro-inflammatory action has been associated with atherosclerosis [50,51], diabetes [52], liver disease [53], and Alzheimer's disease [54]. In addition, high hepatic LPC has

been recently associated with reduced neuronal excitability [55]. Two recent studies report increases of LPC in the brains of mice after mild TBI [56] [57], and that LPC can disturb the function of the blood-brain barrier [58,59]} and the regulation of myelination [60,61].

CE is also produced by the liver and has essential effects on brain cellular signaling, metabolic disease, and inflammation, especially in neurodegeneration [62,63]. Among phosphatidylcholines, ceramides (CER) and hexosylceramides (HCER) were also enriched in probiotic-treated TBI mice's liver. CER and HCER serve many roles in cell membranes, including cellular signaling. Further, levels of CER and HCER have been shown to increase in the plasma after TBI [64–66]. CEs are a storage and transport form of cholesterol and can be found in plasma and lipid droplets. In concordance with this effect, our previous study showed deleterious increases in lipid droplet accumulation in the liver in rodents exposed to TBI [21] [22]. PE and PC are abundant glycerophospholipids phospholipids in mammalian cell membranes [67]. Further, hepatic PE and PC regulate blood lipid and lipoprotein metabolism, oxidative phosphorylation, mitochondrial biogenesis, autophagy, and other energy metabolism functions, playing important regulatory roles in health and disease [68–71]. 16 different species of PEs were enriched among untreated TBI mice, while few PCs were enriched in both treated and untreated TBI mice (see Table 1). We found that glycerophospholipids were enriched in the liver of treated and untreated TBI mice, and these lipids have been shown to increase in the blood of brain trauma patients and to associate with trauma severity [72,73]. Further, our analyses suggest that the probiotic treatment was not sufficient to completely protect the liver from the lipid alterations induced by TBI, as did not fully restore the lipid profile to a normal or adaptive state. However, the probiotic treatment exhibited a dual effect on liver lipid metabolism: it partially reversed some TBI-induced lipid alterations towards sham-like levels, while also generating a distinct set of liver lipids. This indicates that the probiotics had some protective effects but also induced unique changes in the liver lipid profile.

Studies indicate specific roles for gut bacteria in the regulation of systemic lipid metabolism that could be mediated through the production of bacterial metabolites such as SCFAs, secondary bile acids, and trimethylamine – all of which have been shown to act on the liver [74,75]. Other studies have also demonstrated a direct link between gut bacteria and its products to hepatic lipid metabolism [76,77]. Yoo et al. showed that probiotics comprised of specific *Lactobacillus* strains could produce changes in lipid metabolism in the liver, reducing hepatic fat accumulation, cholesterol, and triglycerides, decreasing lipogenesis and increasing fat oxidation [77]. Kindt et al. used a multi-omics approach to compare germ-free and specific pathogen-free (SPF) mice whose gut microbiota was manipulated by selective antibiotics [76]. They showed gut microbiota-dependent changes in liver lipidomic profiles relevant to the biophysical properties of cell membranes, cellular signaling, host metabolism, and inflammation. Our data suggest a potentially injurious decoupling of gut bacteria and hepatic lipids after TBI, where a probiotic treatment conferred partial protection of the hepatic lipid metabolism.

Our preemptive approach provides insights into the potential protective effects of probiotics. Future studies should aim to experiment under conditions where probiotic treatment is started after TBI surgery to better mimic clinical scenarios and evaluate the therapeutic

potential of probiotics in treating TBI. Further, we utilized only male C57/BL6 mice to maintain consistency and reduce variability, given our small sample sizes. Our previous research has shown sex-dependent effects in probiotic treatments and TBI models [78]. Limiting our study to males helps control for these variables. However, we acknowledge this limitation and recommend including both sexes in future studies to explore potential sex-specific responses to probiotic treatment in TBI models.

In conclusion, our research indicates that TBI can cause disturbances in the gut microbiota, disrupt the metabolism of lipids in the liver, and affect the communication between the gut and the liver. The findings suggest that manipulating or modifying the composition of gut bacteria might be possible to protect the brain, behavior, and liver metabolism from the adverse effects of TBI. Furthermore, our study highlights the intricate interplay between gut microbiota and liver lipids that can impact brain function and plasticity in TBI development. Probiotic treatment could have the potential to modify the processes leading to the TBI pathology. Overall, our study suggests that by understanding and intervening in the gut-brain-liver axis, researchers and medical practitioners could develop strategies to improve outcomes for individuals affected by TBI.

Supplementary Material

Refer to Web version on PubMed Central for supplementary material.

Funding

This work was supported by National Institutes of Health (NIH) grants R01-NS111378, and R01-NS116383 (FGP), and NIH grant R56AG080920 (SV) from the National Institute on Aging (NIA).

Data availability

Data will be made available on request.

References

[1]. Capizzi A, Woo J, Verduzco-Gutierrez M, Traumatic brain injury: an overview of epidemiology, pathophysiology, and medical management, Med. Clin. North Am 104 (2) (2020) 213–238. [PubMed: 32035565]

[2]. Mercado NM, et al. , Traumatic brain injury alters the gut-derived serotonergic system and associated peripheral organs, Biochim. Biophys. Acta Mol. basis Dis 1868 (11) (2022) 166491. [PubMed: 35902006]

[3]. Barlow B, et al. , Targeting the gut microbiome in the management of sepsis-associated encephalopathy, Front. Neurol 13 (2022) 999035. [PubMed: 36247756]

[4]. Cryan JF, O'Mahony SM, The microbiome-gut-brain axis: from bowel to behavior, Neurogastroenterol. Motil 23 (3) (2011) 187–192. [PubMed: 21303428]

[5]. Sundman MH, et al. , The bidirectional gut-brain-microbiota axis as a potential nexus between traumatic brain injury, inflammation, and disease, Brain Behav. Immun 66 (2017) 31–44. [PubMed: 28526435]

[6]. Liu X, Cao S, Zhang X, Modulation of gut microbiota-brain axis by probiotics, prebiotics, and diet, J. Agric. Food Chem. 63 (36) (2015) 7885–7895. [PubMed: 26306709]

[7]. Chen Z, et al. , Gut microbiota: therapeutic targets of ginseng against multiple disorders and ginsenoside transformation, Front. Cell. Infect. Microbiol 12 (2022) 853981. [PubMed: 35548468]

[8]. Zhou Y, et al. , Gut microbiota changes and their correlation with cognitive and neuropsychiatric symptoms in Alzheimer's disease, J. Alzheimers Dis. 81 (2) (2021) 583–595. [PubMed: 33814442]

[9]. Cheng LH, et al. , Psychobiotics in mental health, neurodegenerative and neurodevelopmental disorders, J. Food Drug Anal 27 (3) (2019) 632–648. [PubMed: 31324280]

[10]. Czajeczny D, Kabzinska K, Wojciak RW, Effects of Bifidobacterium Lactis BS01 and Lactobacillus acidophilus LA02 on cognitive functioning in healthy women, Appl. Neuropsychol. Adult (2021) 1–9.

[11]. Ruiz-Gonzalez C, et al. , Effects of probiotics supplementation on dementia and cognitive impairment: a systematic review and meta-analysis of preclinical and clinical studies, Prog. Neuro-Psychopharmacol. Biol. Psychiatry 108 (2021) 110189.

[12]. Kruger JF, et al. , Probiotics for dementia: a systematic review and meta-analysis of randomized controlled trials, Nutr. Rev 79 (2) (2021) 160–170. [PubMed: 32556236]

[13]. Rianda D, et al. , Effect of probiotic supplementation on cognitive function in children and adolescents: a systematic review of randomised trials, Benefic. Microbes 10 (8) (2019) 873–882.

[14]. Akbari E, et al. , Effect of probiotic supplementation on cognitive function and metabolic status in Alzheimer's disease: a randomized, double-blind and controlled trial, Front. Aging Neurosci. 8 (2016) 256. [PubMed: 27891089]

[15]. Goudarzvand M, et al. , Probiotics Lactobacillus plantarum and bifidobacterium B94: cognitive function in demyelinated model, Med. J. Islam Repub. Iran 30 (2016) 391. [PubMed: 27579282]

[16]. Steenbergen L, et al. , A randomized controlled trial to test the effect of multispecies probiotics on cognitive reactivity to sad mood, Brain Behav. Immun. 48 (2015) 258–264. [PubMed: 25862297]

[17]. Zhang M, et al. , Bidirectional interaction of nobiletin and gut microbiota in mice fed with a high-fat diet, Food Funct. 12 (8) (2021) 3516–3526. [PubMed: 33900329]

[18]. Knudsen C, et al. , Hepatoprotective effects of indole, a gut microbial metabolite, in leptin-deficient obese mice, J. Nutr. 151 (6) (2021) 1507–1516. [PubMed: 33693866]

[19]. Monteiro-Cardoso VF, Corliano M, Singaraja RR, Bile acids: a communication channel in the gut-brain axis, NeuroMolecular Med. 23 (1) (2021) 99–117. [PubMed: 33085065]

[20]. Li B, et al. , Metabolite identification in fecal microbiota transplantation mouse livers and combined proteomics with chronic unpredictive mild stress mouse livers, Transl. Psychiatry 8 (1) (2018) 34. [PubMed: 29382834]

[21]. Rege SD, et al. , Brain trauma disrupts hepatic lipid metabolism: blame it on fructose? Mol. Nutr. Food Res. 63 (15) (2019) e1801054. [PubMed: 31087499]

[22]. Khandelwal M, et al. , Liver acts as a metabolic gate for the traumatic brain injury pathology: protective action of thyroid hormone, Biochim. Biophys. Acta Mol. basis Dis 1869 (6) (2023) 166728. [PubMed: 37137432]

[23]. Ghazalpour A, et al. , Expanding role of gut microbiota in lipid metabolism, Curr. Opin. Lipidol. 27 (2) (2016) 141–147. [PubMed: 26855231]

[24]. Victor DW 3rd, Quigley EM, Microbial therapy in liver disease: probiotics probe the microbiome-gut-liver-brain axis, Gastroenterology 147 (6) (2014) 1216–1218. [PubMed: 25457846]

[25]. Hertz FB, et al. , Effects of antibiotics on the intestinal microbiota of mice, Antibiotics (Basel) 9 (4) (2020).

[26]. Namdar I, et al. , Motor effects of minimal traumatic brain injury in mice, J. Mol. Neurosci. 70 (3) (2020) 365–377. [PubMed: 31820347]

[27]. Callahan BJ, et al. , DADA2: high-resolution sample inference from Illumina amplicon data, Nat. Methods 13 (7) (2016) 581–583. [PubMed: 27214047]

[28]. Katoh K, et al. , MAFFT: a novel method for rapid multiple sequence alignment based on fast Fourier transform, Nucleic Acids Res. 30 (14) (2002) 3059–3066. [PubMed: 12136088]

[29]. Price MN, Dehal PS, Arkin AP, FastTree 2–approximately maximum-likelihood trees for large alignments, PLoS One 5 (3) (2010) e9490. [PubMed: 20224823]

[30]. Wang Q, et al. , Naive Bayesian classifier for rapid assignment of rRNA sequences into the new bacterial taxonomy, Appl. Environ. Microbiol. 73 (16) (2007) 5261–5267. [PubMed: 17586664]

[31]. Lozupone CA, et al. , Quantitative and qualitative beta diversity measures lead to different insights into factors that structure microbial communities, Appl. Environ. Microbiol. 73 (5) (2007) 1576–1585. [PubMed: 17220268]

[32]. Lozupone C, Knight R, UniFrac: a new phylogenetic method for comparing microbial communities, Appl. Environ. Microbiol. 71 (12) (2005) 8228–8235. [PubMed: 16332807]

[33]. Bligh EG, Dyer WJ, A rapid method of total lipid extraction and purification, Can. J. Biochem. Physiol. 37 (8) (1959) 911–917. [PubMed: 13671378]

[34]. Mallick H, et al. , Multivariable association discovery in population-scale meta-omics studies, PLoS Comput. Biol. 17 (11) (2021) e1009442. [PubMed: 34784344]

[35]. Leung K, Thuret S, Gut microbiota: a modulator of brain plasticity and cognitive function in ageing, Healthcare (Basel) 3 (4) (2015) 898–916. [PubMed: 27417803]

[36]. Mohammadi G, et al. , Probiotic mixture of Lactobacillus helveticus R0052 and Bifidobacterium longum R0175 attenuates hippocampal apoptosis induced by lipopolysaccharide in rats, Int. Microbiol 22 (3) (2019) 317–323. [PubMed: 30810993]

[37]. Griesbach GS, Gomez-Pinilla F, Hovda DA, The upregulation of plasticity-related proteins following TBI is disrupted with acute voluntary exercise, Brain Res. 1016 (2) (2004) 154–162. [PubMed: 15246851]

[38]. Griesbach GS, Hovda DA, Gomez-Pinilla F, Exercise-induced improvement in cognitive performance after traumatic brain injury in rats is dependent on BDNF activation, Brain Res. 1288 (2009) 105–115. [PubMed: 19555673]

[39]. Griesbach GS, et al. , Alterations in BDNF and synapsin I within the occipital cortex and hippocampus after mild traumatic brain injury in the developing rat: reflections of injury-induced neuroplasticity, J. Neurotrauma 19 (7) (2002) 803–814. [PubMed: 12184851]

[40]. Monsalve FA, et al. , Peroxisome proliferator-activated receptor targets for the treatment of metabolic diseases, Mediat. Inflamm 2013 (2013) 549627.

[41]. Mazziotta C, et al. , Probiotics mechanism of action on immune cells and beneficial effects on human health, Cells 12 (1) (2023).

[42]. Messaoudi M, et al. , Beneficial psychological effects of a probiotic formulation (Lactobacillus helveticus R0052 and Bifidobacterium longum R0175) in healthy human volunteers, Gut Microbes 2 (4) (2011) 256–261. [PubMed: 21983070]

[43]. Taverniti V, et al. , Probiotics modulate mouse gut microbiota and influence intestinal immune and serotonergic gene expression in a site-specific fashion, Front. Microbiol 12 (2021) 706135. [PubMed: 34539604]

[44]. Treangen TJ, et al. , Traumatic brain injury in mice induces acute bacterial dysbiosis within the fecal microbiome, Front. Immunol. 9 (2018) 2757. [PubMed: 30546361]

[45]. Curry KD, et al. , Emu: species-level microbial community profiling of full-length 16S rRNA Oxford nanopore sequencing data, Nat. Methods 19 (7) (2022) 845–853. [PubMed: 35773532]

[46]. Tian B, et al. , Lycium ruthenicum anthocyanins attenuate high-fat diet-induced colonic barrier dysfunction and inflammation in mice by modulating the gut microbiota, Mol. Nutr. Food Res. 65 (8) (2021) e2000745. [PubMed: 33629483]

[47]. Markovic M, et al. , Lipids and lipid-processing pathways in drug delivery and therapeutics, Int. J. Mol. Sci 21 (9) (2020).

[48]. Lee YK, et al. , Lysophosphatidylcholine, oxidized low-density lipoprotein and cardiovascular disease in Korean hemodialysis patients: analysis at 5 years of follow-up, J. Korean Med. Sci 28 (2) (2013) 268–273. [PubMed: 23400766]

[49]. Sugasini D, et al. , Enrichment of brain docosahexaenoic acid (DHA) is highly dependent upon the molecular carrier of dietary DHA: lysophosphatidylcholine is more efficient than either phosphatidylcholine or triacylglycerol, J. Nutr. Biochem 74 (2019) 108231. [PubMed: 31665653]

[50]. Zhou Z, et al. , Lipoprotein-derived lysophosphatidic acid promotes atherosclerosis by releasing CXCL1 from the endothelium, Cell Metab. 13 (5) (2011) 592–600. [PubMed: 21531341]

[51]. Zhou X, et al. , Identification of lysophosphatidylcholines and sphingolipids as potential biomarkers for acute aortic dissection via serum metabolomics, Eur. J. Vasc. Endovasc. Surg. 57 (3) (2019) 434–441. [PubMed: 30087010]

[52]. Drzazga A, et al. , Lysophosphatidylcholine and its phosphorothioate analogues potentiate insulin secretion via GPR40 (FFAR1), GPR55 and GPR119 receptors in a different manner, Mol. Cell. Endocrinol. 472 (2018) 117–125. [PubMed: 29225068]

[53]. Kakisaka K, et al. , Caspase-independent hepatocyte death: a result of the decrease of lysophosphatidylcholine acyltransferase 3 in non-alcoholic steatohepatitis, J. Gastroenterol. Hepatol. 34 (7) (2019) 1256–1262. [PubMed: 30160786]

[54]. Grimm MO, et al. , From brain to food: analysis of phosphatidylcholins, lyso-phosphatidylcholins and phosphatidylcholin-plasmalogens derivates in Alzheimer's disease human post mortem brains and mice model via mass spectrometry, J. Chromatogr. A 1218 (42) (2011) 7713–7722. [PubMed: 21872257]

[55]. Fischer C, et al. , Prevention of age-associated neuronal hyperexcitability with improved learning and attention upon knockout or antagonism of LPAR2, Cell. Mol. Life Sci. 78 (3) (2021) 1029–1050. [PubMed: 32468095]

[56]. Ojo JO, et al. , Converging and differential brain phospholipid dysregulation in the pathogenesis of repetitive mild traumatic brain injury and Alzheimer's disease, Front. Neurosci. 13 (2019) 103. [PubMed: 30837829]

[57]. Palafox-Sanchez V, et al. , The interaction between brain and liver regulates lipid metabolism in the TBI pathology, Biochim. Biophys. Acta Mol. basis Dis 1867 (4) (2021) 166078. [PubMed: 33444711]

[58]. Qiao J, et al. , Lysophosphatidylcholine impairs endothelial barrier function through the G protein-coupled receptor GPR4, Am. J. Phys. Lung Cell. Mol. Phys. 291 (1) (2006) L91–101.

[59]. Muramatsu R, et al. , Prostacyclin prevents pericyte loss and demyelination induced by lysophosphatidylcholine in the central nervous system, J. Biol. Chem. 290 (18) (2015) 11515–11525. [PubMed: 25795781]

[60]. Plemel JR, et al. , Mechanisms of lysophosphatidylcholine-induced demyelination: a primary lipid disrupting myelinopathy, Glia 66 (2) (2018) 327–347. [PubMed: 29068088]

[61]. Ou Z, et al. , Olig2-targeted G-protein-coupled receptor Gpr17 regulates oligodendrocyte survival in response to lysolecithin-induced demyelination, J. Neurosci. 36 (41) (2016) 10560–10573. [PubMed: 27733608]

[62]. Liu L, et al. , The glia-neuron lactate shuttle and elevated ROS promote lipid synthesis in neurons and lipid droplet accumulation in glia via APOE/D, Cell Metab. 26 (5) (2017) 719–737.e6. [PubMed: 28965825]

[63]. Liu L, et al. , Glial lipid droplets and ROS induced by mitochondrial defects promote neurodegeneration, Cell 160 (1–2) (2015) 177–190. [PubMed: 25594180]

[64]. Anyaegbu CC, et al. , Plasma lipid profiles change with increasing numbers of mild traumatic brain injuries in rats, Metabolites 12 (4) (2022).

[65]. Huguenard CJC, et al. , Plasma lipidomic analyses in cohorts with mTBI and/or PTSD reveal lipids differentially associated with diagnosis and APOE epsilon4 carrier status, Front. Physiol 11 (2020) 12. [PubMed: 32082186]

[66]. Thomas I, et al. , Serum metabolome associated with severity of acute traumatic brain injury, Nat. Commun. 13 (1) (2022) 2545. [PubMed: 35538079]

[67]. Tijburg LB, Geelen MJ, van Golde LM, Regulation of the biosynthesis of triacylglycerol, phosphatidylcholine and phosphatidylethanolamine in the liver, Biochim. Biophys. Acta 1004 (1) (1989) 1–19. [PubMed: 2663077]

[68]. Imaizumi K, et al. , The contrasting effect of dietary phosphatidylethanolamine and phosphatidylcholine on serum lipoproteins and liver lipids in rats, J. Nutr. 113 (12) (1983) 2403–2411. [PubMed: 6686250]

[69]. van der Veen JN, et al. , The critical role of phosphatidylcholine and phosphatidylethanolamine metabolism in health and disease, Biochim. Biophys. Acta Biomembr. 1859 (9 Pt B) (2017) 1558–1572. [PubMed: 28411170]

[70]. Wallner S, et al. , Phosphatidylcholine and phosphatidylethanolamine plasmalogens in lipid loaded human macrophages, PLoS One 13 (10) (2018) e0205706. [PubMed: 30308051]

[71]. Calzada E, Onguka O, Claypool SM, Phosphatidylethanolamine metabolism in health and disease, Int. Rev. Cell Mol. Biol. 321 (2016) 29–88.

[72]. Nessel I, Michael-Titus AT, Lipid profiling of brain tissue and blood after traumatic brain injury: a review of human and experimental studies, Semin. Cell Dev. Biol. 112 (2021) 145–156. [PubMed: 33036880]

[73]. Gier EC, et al. , Lipidome alterations following mild traumatic brain injury in the rat, Metabolites 12 (2) (2022).

[74]. Ghazalpour A, et al. , Genetic regulation of mouse liver metabolite levels, Mol. Syst. Biol. 10 (5) (2014) 730. [PubMed: 24860088]

[75]. Schoeler M, Caesar R, Dietary lipids, gut microbiota and lipid metabolism, Rev. Endocr. Metab. Disord 20 (4) (2019) 461–472. [PubMed: 31707624]

[76]. Kindt A, et al. , The gut microbiota promotes hepatic fatty acid desaturation and elongation in mice, Nat. Commun. 9 (1) (2018) 3760. [PubMed: 30218046]

[77]. Yoo SR, et al. , Probiotics L. plantarum and L. curvatus in combination alter hepatic lipid metabolism and suppress diet-induced obesity, Obesity (Silver Spring) 21 (12) (2013) 2571–2578. [PubMed: 23512789]

[78]. Holcomb M, et al. , Probiotic treatment causes sex-specific neuroprotection after traumatic brain injury in mice, Res Sq (2024), 10.21203/rs.3.rs-4196801/v1 [Preprint].

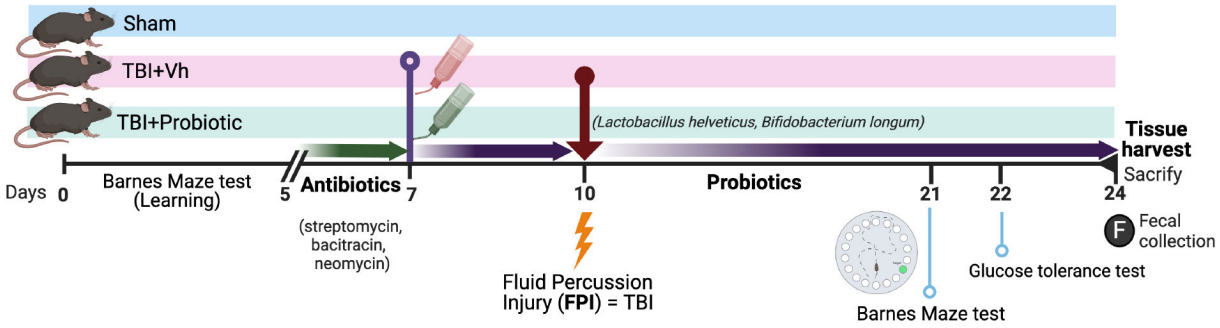

Fig. 1. Study Timeline Overview.

Mice were trained in the Barnes maze, consisting of two daily trials over five consecutive days (days 1–5). Subsequently, all mice received antibiotics in their drinking water for a period of two days (days 5–7) before the initiation of treatment. Probiotic (TBI-Probiotic) or control solutions (TBI-Vh) were initiated the day after antibiotics application and continued until the conclusion of the experiment on day 24. On day 10, three days after starting the probiotic or Vh treatment, mice underwent either Fluid Percussion injury (FPI) or sham surgeries. Behavioral assessments took place one-week post-surgeries on day 21, followed by a glucose tolerance test on the subsequent day (day 22). On day 24, mice were sacrificed (14 days post-TBI), and various body tissues and cecal fecal content were collected for microbiome analysis.

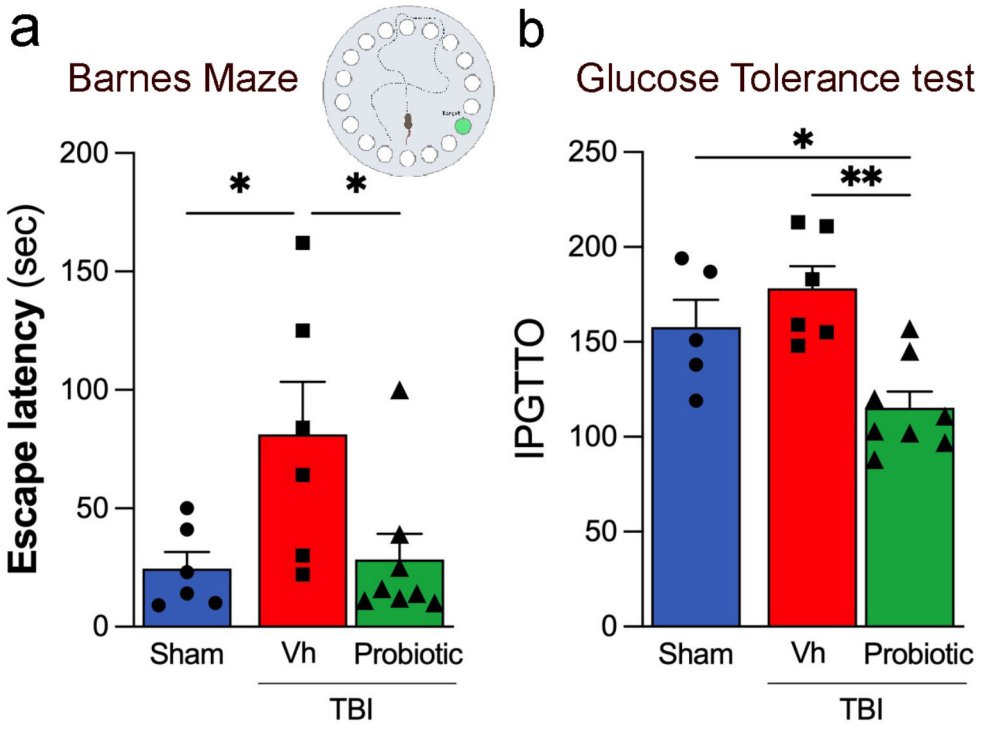

Fig. 2. Probiotic treatment improves memory performance and reduces glucose tolerance after brain injury.

(a) Mice experiencing mild FPI (TBI-Vh) demonstrated increased latency times in locating the escape hole during the Barnes Maze test, compared to the more efficient performance of sham-operated mice. However, TBI mice that received probiotic treatment showed latency times comparable to the sham group, indicating a potential amelioration of memory impairments caused by brain injury. (b) The y-axis represents the area under the curve (AUC) for the intraperitoneal glucose tolerance test (IPGTT). An increased AUC indicates impaired glucose regulation and elevated blood glucose levels, while a decreased AUC indicates enhanced glucose regulation and lower blood glucose levels, signifying a healthier metabolic state. The data demonstrate that TBI mice that received probiotic treatment exhibited a decrease in AUC, compared to both untreated TBI mice and sham-treated mice, suggesting improved glucose tolerance. One-way ANOVA with Tukey's multiple comparison test (*$p < 0.05$, **$p < 0.01$).

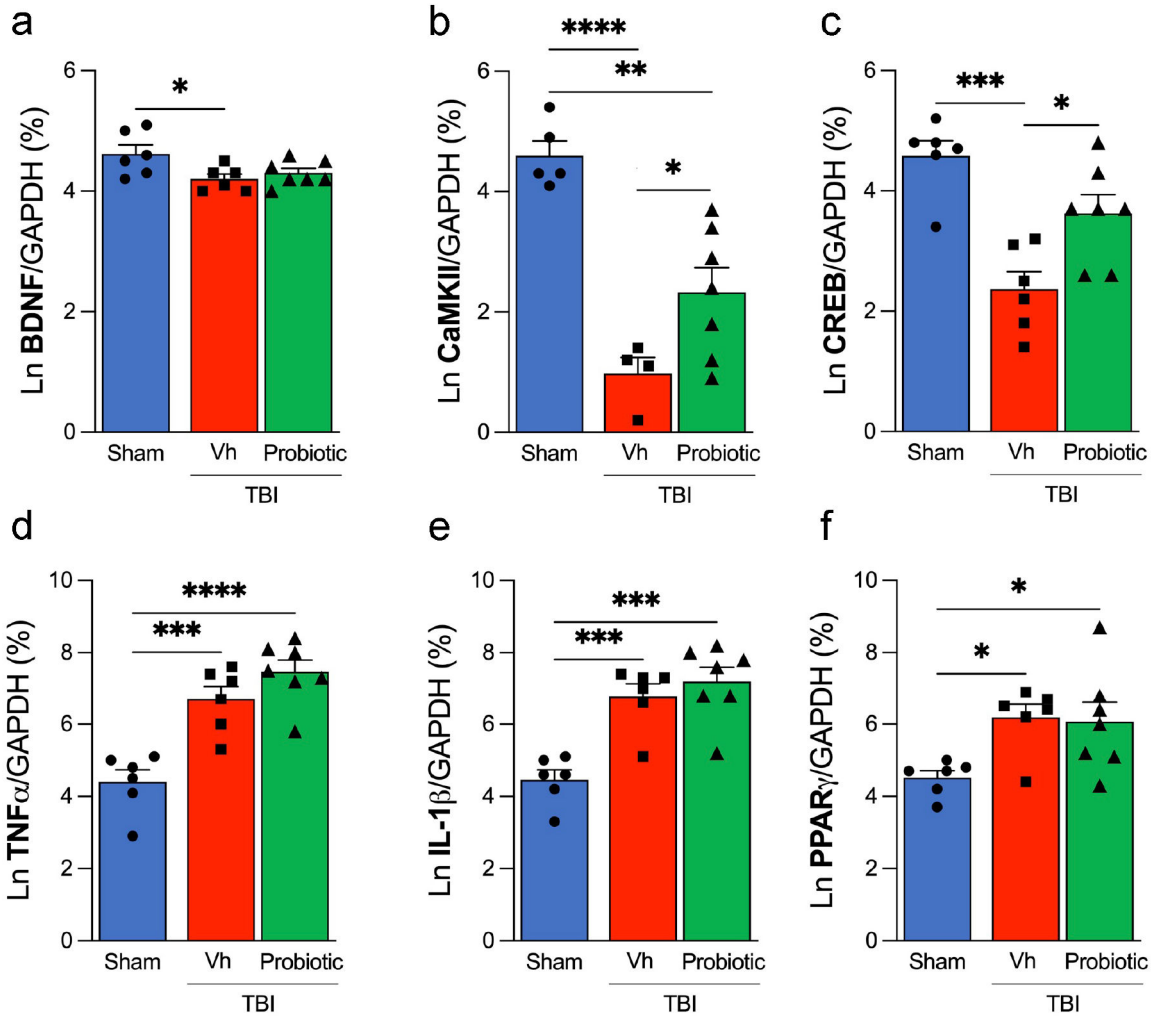

Fig. 3. Changes in gene expression related to hippocampal neuroplasticity and neuroinflammation following traumatic brain injury (TBI).

TBI was associated with a notable decrease in neuroplasticity markers and an increase in neuroinflammatory markers. Probiotic intervention, however, appeared to counteract the negative impacts of brain injury, particularly in the CaMKII/CREB signaling pathway. (a) Post-TBI, there was a reduction in the expression of the BDNF gene, with similar levels observed in both the probiotic-treated and vehicle (Vh) TBI groups. (b) In contrast, a decrease in CaMKII expression due to TBI was lessened by probiotic treatment. (c) CREB expression demonstrated a similar trend, affected by both the injury and probiotic treatment. (d, e) TBI induced an upregulation in the proinflammatory genes TNF-α and IL-1β, which were not significantly altered by probiotic treatment. (f) Changes were also seen in the neuroprotective and anti-inflammatory gene PPAR-γ in the TBI group, with no marked differences between the probiotic and Vh-treated groups. One-way ANOVA with Tukey's multiple comparison test, indicating statistical significance at $*p < 0.05$, $**p < 0.01$, n = 6–8/group.

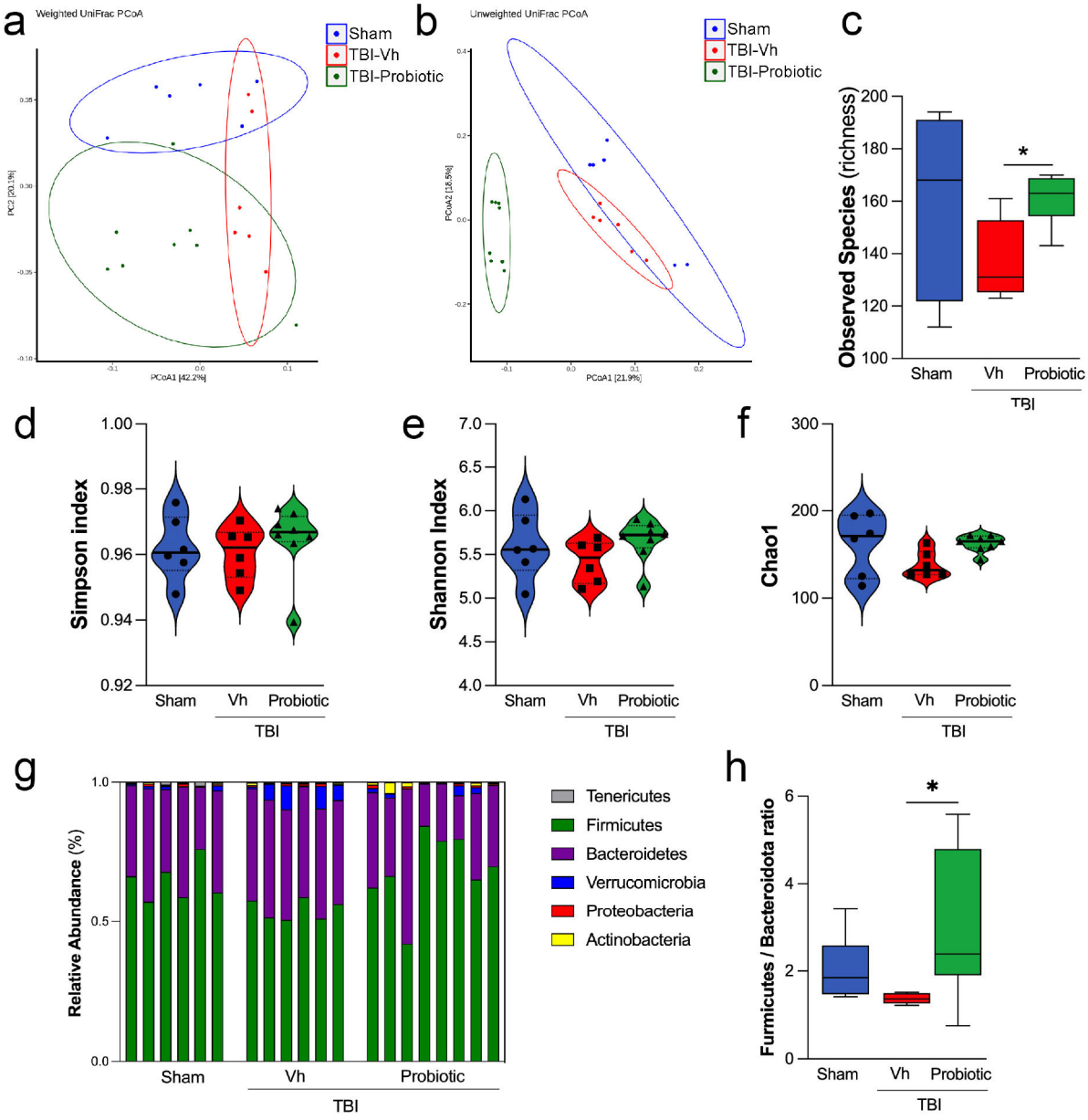

Fig. 4. Impact of Probiotic Treatment on Gut Microbiota Diversity and Composition in a Mouse Model of TBI.

(a) Weighted UniFrac principal coordinates analysis (PCoA) plots showing distinct clustering of gut microbiota communities among sham-operated mice (Sham, blue), TBI mice treated with vehicle (TBI-Vh, red), and TBI mice treated with probiotics (TBI-Probiotic, green). (b) Unweighted UniFrac PCoA plots further illustrate the differences in community structure between the groups. (c) Observed species richness is significantly higher in the Sham group compared to TBI-Vh, with the TBI-Probiotic group showing an intermediate level of species richness (*$p < 0.05$). (d) Simpson index ($p = 0.727$) and (e) Shannon index ($p = 0.303$) violin plots display the biodiversity within each group, indicating no significant differences across treatments. (f) Chao1 estimator plots also reveal similar patterns of species richness among the three groups ($p = 0.101$). (g) Relative abundance

bar plots of major bacterial phyla demonstrate the distribution and proportions within each treatment group, showing the dominance of *Firmicutes* and *Bacteroidetes*. (h) Firmicutes/Bacteroidetes ratio bar plots highlight a significant increase in this ratio in the TBI-Probiotic group compared to the TBI-Vh and Sham groups (*$p < 0.05$).

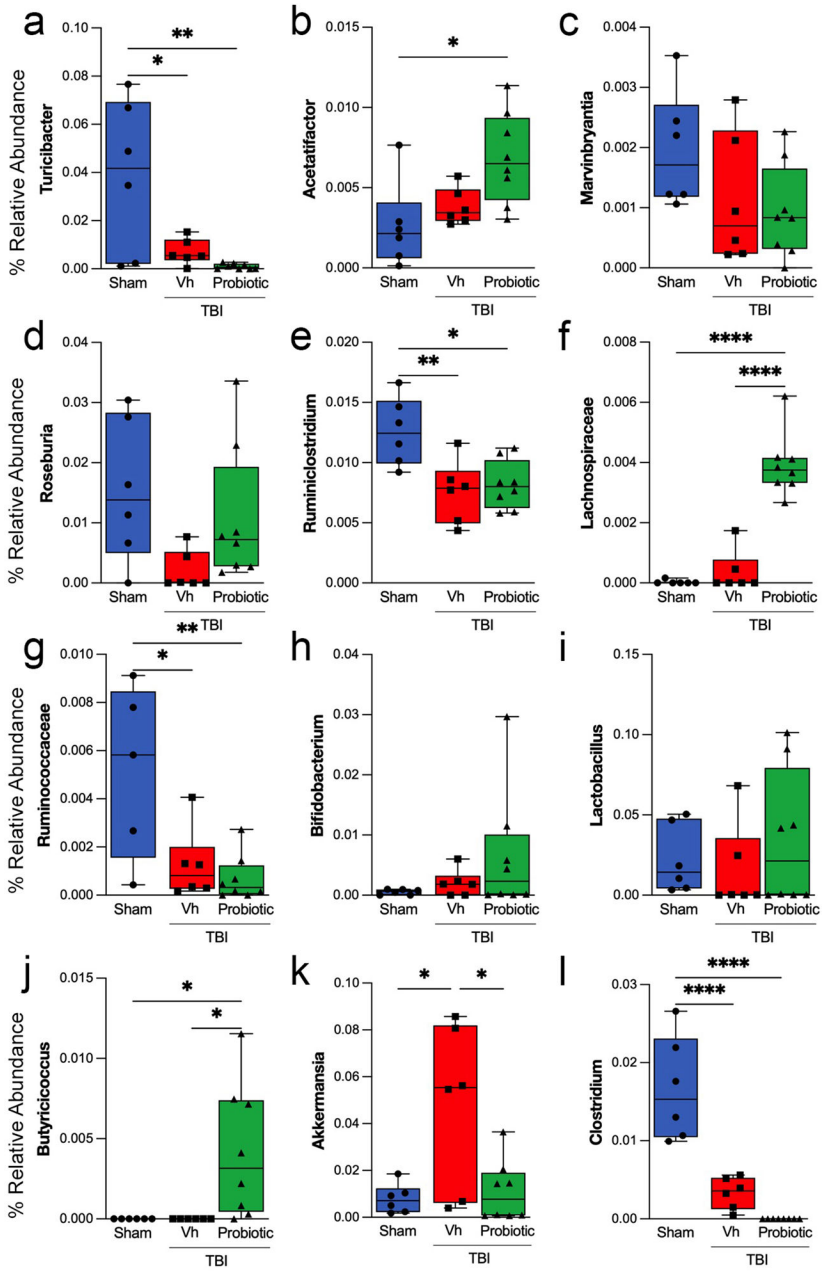

Fig. 5. Changes in Bacterial Genera Following Probiotic Treatment in Mice with Traumatic Brain Injury (TBI).

(a-l) Box plots illustrating the relative abundance of various bacterial genera in sham-operated mice (Sham), mice subjected to TBI treated with vehicle (TBI-Vh), and mice subjected to TBI treated with probiotics (TBI-Probiotic). (a) *Turicibacter* relative abundance are significantly higher in the Sham group compared to both TBI-Vh and TBI-Probiotic groups (*p < 0.05, **p < 0.01). (b) *Acetatifactor* abundance is increased in the TBI-Probiotic group in comparison to the Sham group (*p < 0.05). In contrast, (c) *Marvinbryantia* and (d) Roseburia levels were comparatively stable across all three groups. (e) *Ruminiclostridium* is significantly more abundant in the Sham group relative to TBI-Vh and TBI-Probiotic groups (*p < 0.05, **p < 0.01). (f) *Lachnospiraceae* relative abundance is significantly

increased in the TBI-Probiotic group, with no significant difference between the Sham and TBI-Vh groups (****$p < 0.0001$). (g) *Ruminococcaceae* is significantly more prevalent in the Sham group compared to TBI-Vh and TBI-Probiotic groups (*$p < 0.05$, **$p < 0.01$). (h) *Bifidobacterium* shows no significant difference across the groups. (i) *Lactobacillus* abundance is higher in the TBI-Probiotic group compared to TBI-Vh but shows no significant change. (j) *Butyricicoccus* is increased in the TBI-Probiotic group compared to TBI-Vh and Sham groups (*$p < 0.05$). (k) *Akkermansia* is notably more abundant in the TBI-Vh group, with a significant reduction observed in the Sham and TBI-Probiotic groups (*$p < 0.05$). (l) *Clostridium* levels are dramatically reduced in the TBI-Probiotic group compared to both Sham and TBI-Vh (****$p < 0.0001$).

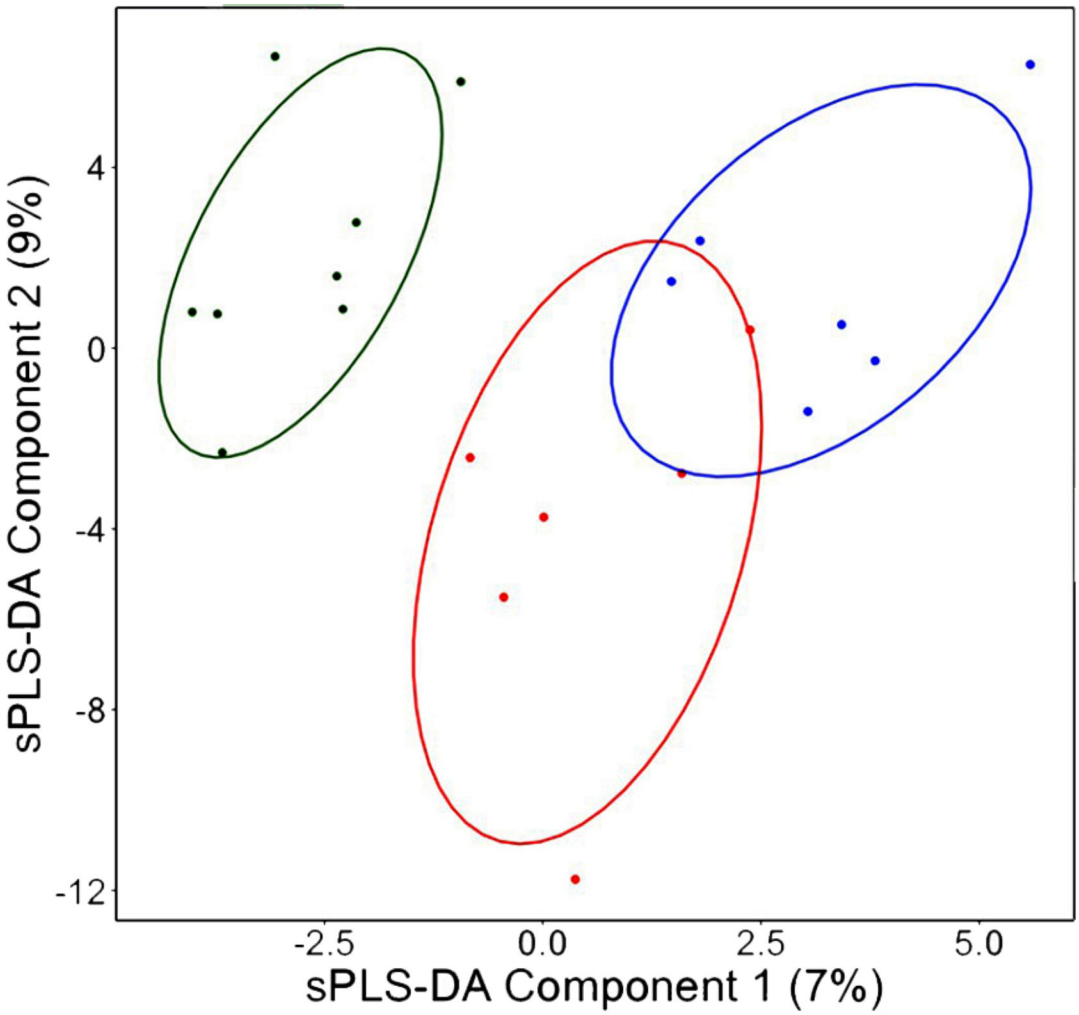

Fig. 6. Differential hepatic lipid profiles among experimental groups.

The Sparse Partial Least Squares Discriminatory Analysis (sPLS-DA) multivariate technique was used to delineate two principal components (represented along the X- and Y-variate axes) that capture the variance in hepatic lipid changes. This scatter plot displays the segregation of hepatic lipid profiles among distinct experimental conditions as discerned by sPLS-DA. Each dot represents an individual sample plotted against the first and second sPLS-DA components, which explain 7 % and 9 % of the variance, respectively. The first component effectively separates the sham (blue) and probiotic-treated (green) samples, while the second component is distinctive for the TBI vehicle (Vh) (red) samples. The clustering of dots within the ellipses indicates the lipidomic signature unique to each experimental group, with the minimal overlap between ellipses signifying clear distinctions in lipid composition. The ellipses are drawn to encapsulate the 95 % confidence interval for each group, illustrating the robust differentiation achieved by sPLS-DA in profiling hepatic lipids. The first sPLS-DA component reflects the influence of TBI-probiotic intervention rises to a unique lipid sub-profile when compared to both sham and TBI-Vh conditions. Furthermore, the second component accounts for 47.0 % of the variability and captures the effects of TBI and probiotic treatment. Notably, the impact of TBI on the second sPLS-DA

component appears to be mitigated by the probiotic treatment, as suggested by the inverse beta coefficients of similar magnitude.

Table 1.

Main contributors to Discriminant Analysis of hepatic lipids

Sham Control	DA score	TBI	DA score	TBI+Probiotic	DA score
CE(22:2)	0.100	CE(18:2)	0.253	CER(16:0)	0.207
FFA(24:1)	0.136	CE(20:3)	0.128	CER(18:0)	0.222
PC(16:0/20:4)	0.126	LPC(16:1)	0.128	HCER(22:0)	0.169
TAG46:2-FA12:0	0.321	PC(14:0/16:1)	0.224	PC(16:0/18:0)	0.257
TAG47:0-FA17:0	0.118	PC(14:0/18:1)	0.122	PC(18:0/16:1)	0.184
TAG48:3-FA12:0	0.360	PC(16:0/14:0)	0.224	PC(18:0/18:1)	0.449
TAG48:4-FA12:0	0.410	PE(16:0/16:1)	0.132	PC(18:0/20:2)	0.242
TAG53:4-FA20:4	0.158	PE(16:0/18:1)	0.212		
		PE(16:0/18:3)	0.245		
		PE(16:0/20:4)	0.122		
		PE(16:0/22:4)	0.172		
		PE(18:0/16:0)	0.166		
		PE(18:1/16:1)	0.116		
		PE(18:1/22:4)	0.163		
		PE(18:2/16:1)	0.133		
		PE(O–16:0/22:4)	0.163		
		PE(O–18:0/18:1)	0.172		
		PE(P-16:0/20:4)	0.123		
		PE(P-16:0/22:4)	0.154		
		PE(P-18:0/20:4)	0.113		
		PE(P-18:1/20:3)	0.121		
		PE(P-18:1/20:4)	0.194		
		TAG49:3-FA18:2	0.134		
		TAG50:5-FA14:1	0.162		

Lipids ordered by class; DA scores were adjusted to show magnitude, not direction; lipids selected exhibited DA scores > 0.10.